Clustering in Neutron-rich Nuclei

H.Horiuchi RCNP
Osaka Univ.

1. Introduction
2. Di-cluster core + neutrons
3. Di-neutron cluster
4. Multi-cluster core + neutrons
5. Summarizing discussion

RIA Theory Meeting, Argonne, 4-7 April ‘06

１. Introduction

neutron-rich nuclei

⇩

neutron skin, neutron halo
(weakly-bound neutrons with dilute density)

⇩

correlations and clustering
due to weakly bound dilute neutrons

Here, two kinds of clustering generated or supported by excess neutrons

1. α **cluster structure**
   two-cluster structure
   multi-cluster structure
2. **formation of di-neutron clusters**

2. Di-cluster core + neutrons

Ab initio calculation with
realistic nuclear force

**Wiringer,Pieper,
Carlson,
Pandharipande**

P.R.C. 62, 014001
(2000)

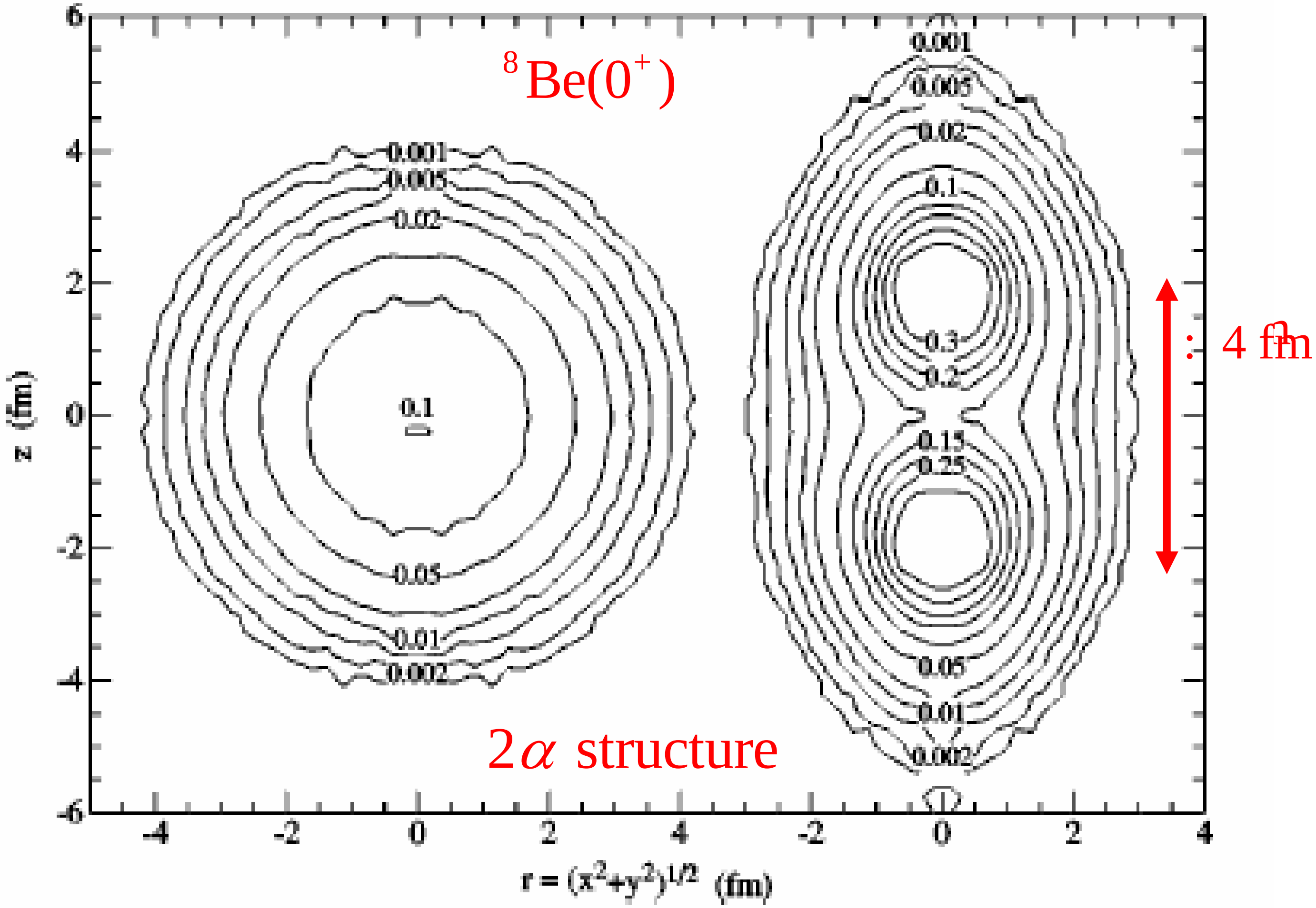

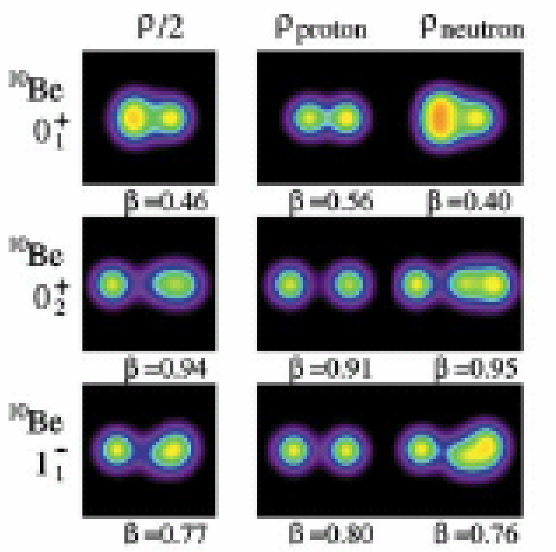

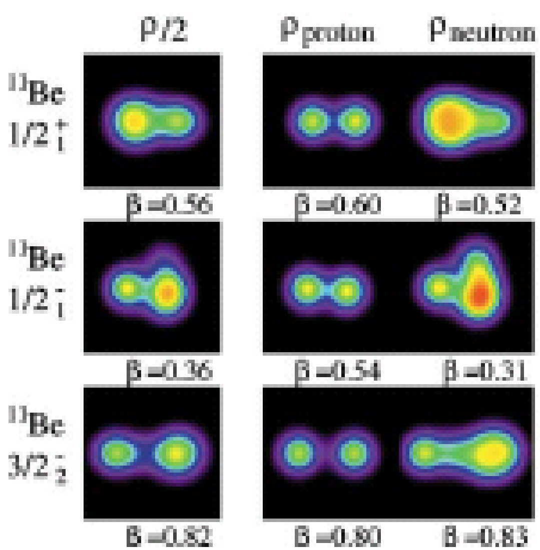

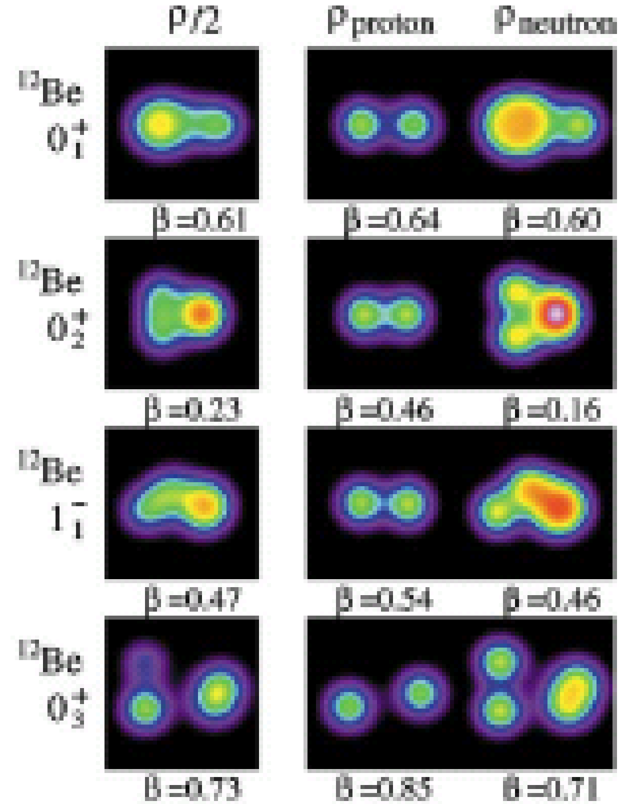

AMD (antisymmetrized molecular dynamics)

VAP calculation

Density distribution of the intrinsic states

C.R.Physique 4(‘03), 497

Kanada-En’yo et al.

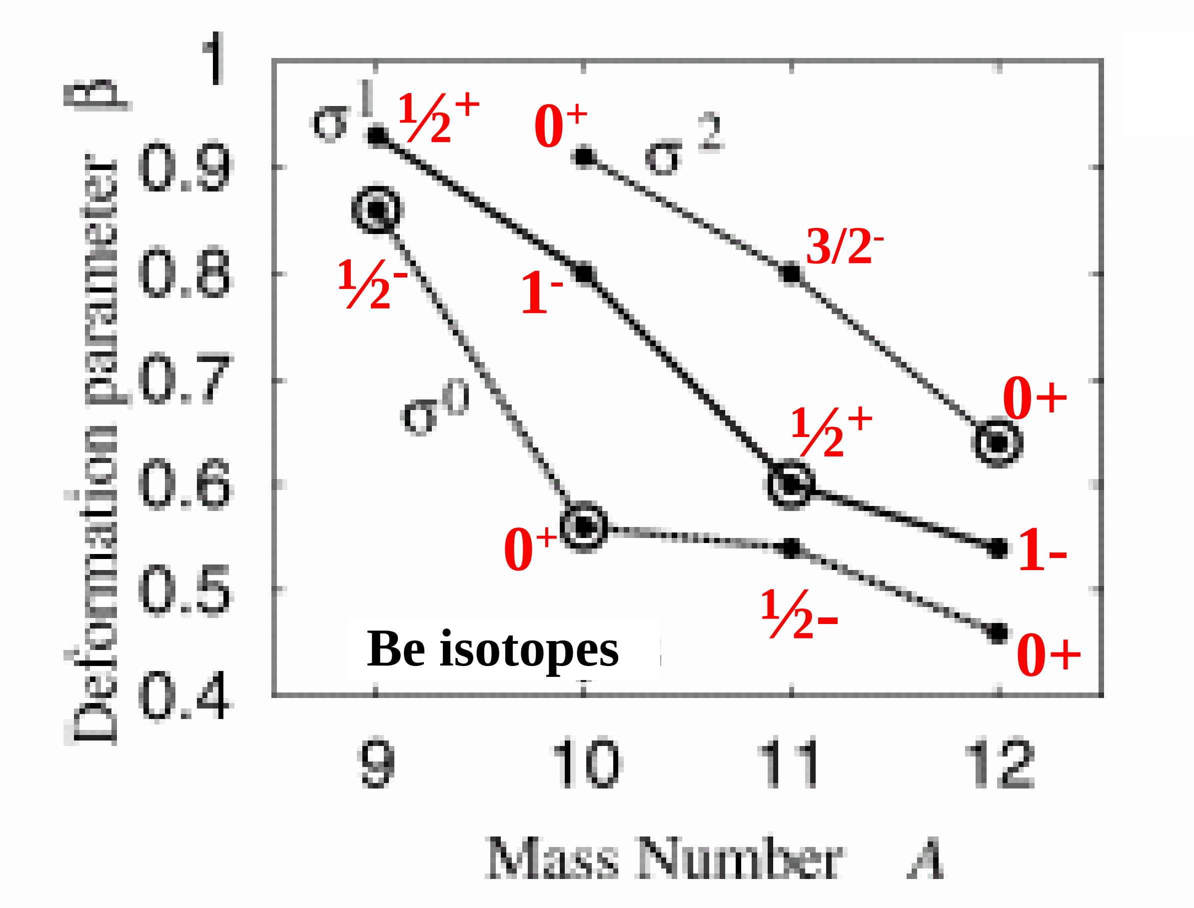

⊙ ground states

Shell inversion for ^{11}Be and ^{12}Be

Kanada-En'yo et al.

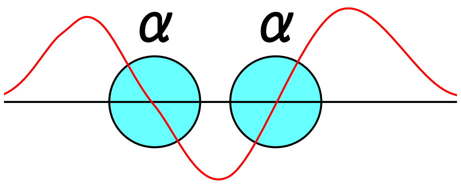

σ -orbit (sd-orbit)

σ -orbit sustains or enhances clustering

^{10}Be

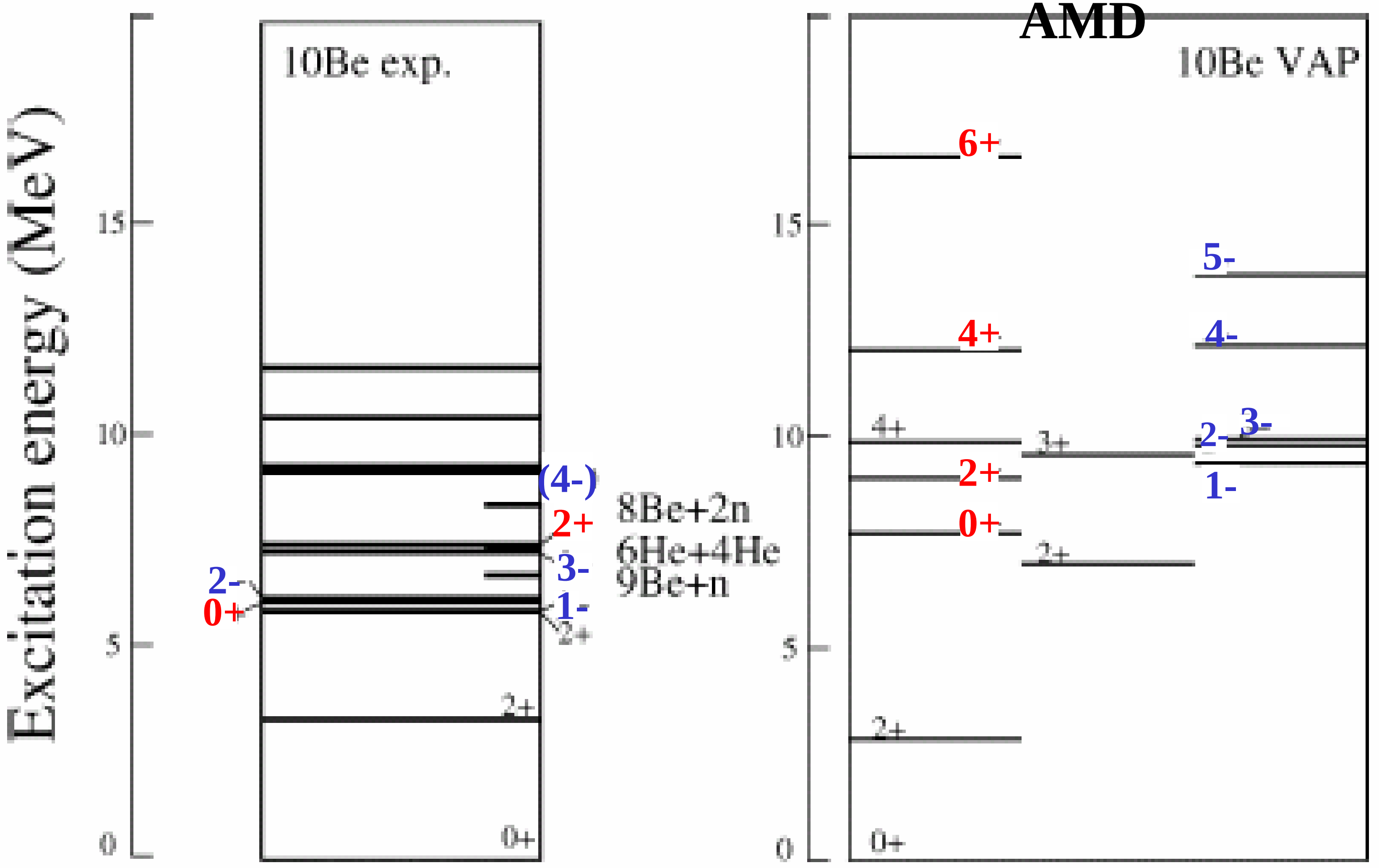

Kanada-En' yo et al.

Kanada-En’yo et al.

○ : AMD calculation + : experiments

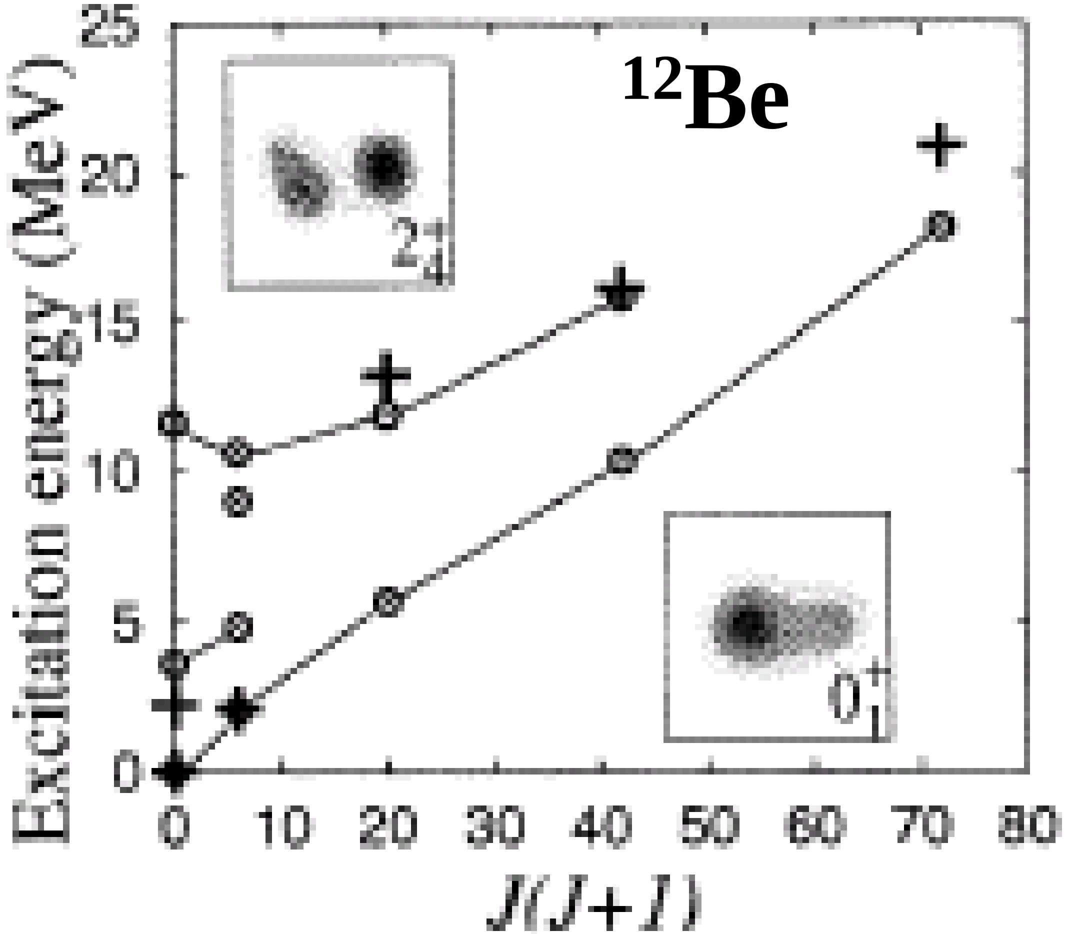

^{6}He-^{6}He molecule

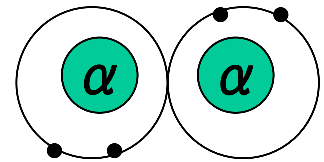

(atomic orbits)

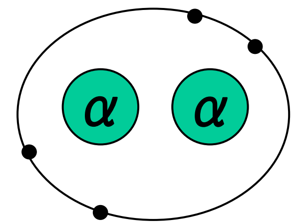

molecular orbits

Observation of shell-model-like 0_2^+

S. Shimoura, et al., Phys.Lett. **560B**, 31 (2003)

Observation of molecular band

M. Freer, et al., Phys. Rev. Lett. **82**, 1383 (1999)

M. Freer, et al., Phys. Rev. C **63**, 034301 (2001)

Table X. $E2$ and $E1$ transition strength. The theoretical results of VAP calculations with the case (g) are compared with the experimental data.[58] The shell model calculations are quoted from the work with the $(0+2)\hbar\omega$ shell model in Ref. 59).

transitions	Mult	exp	present VAP	shell model
^{10}Be;$2_1^+ \to 0_1^+$	$E2$	10.5±1.1 (e fm^2)	11 (e fm^2)	16.26 (e fm^2)
^{10}Be;$0_2^+ \to 2_1^+$	$E2$	3.3±2.0 (e fm^2)	0.6 (e fm^2)	7.20 (e fm^2)
^{10}Be;$0_2^+ \to 1_1^-$	$E1$	1.3±0.6×10^{-2} (e fm)	0.6×10^{-2}(e fm)	
^{10}C;$2_1^+ \to 0_1^+$	$E2$	12.3±2.0 (e fm^2)	9 (e fm^2)	15.22 (e fm^2)

Table XI. B(GT) values of β decays which are the square of the expectation values of Gamow-Teller operator. The experimental data are the values[a] deduced from the cross sections of ^{10}B(t,^{3}He)^{10}Be* at 0° forward angle[54] and the one[b] from Ref. 60). The theoretical results are obtained with the case (g) and the case (h) interactions for ^{10}Be and ^{10}B.

exp initial (J^π, E_x) (MeV)	final (J^π, E_x) (MeV)	B(GT)
^{10}B(3$^+$,0)	^{10}Be(2_1^+,3.37)	0.08± 0.03[a]
^{10}B(3$^+$,0)	^{10}Be(2_2^+,5.96)	0.95± 0.13[a]
^{10}B(3$^+$,0)	^{10}Be(2$^+$ or 3$^+$, 9.4)	0.31± 0.08[a]
^{10}C(0$^+$,0)	^{10}B(1$^+$, 0.72)	3.44 [b]

initial	final	cal (g)	cal (h)
^{10}B(3$^+$)	^{10}Be(2_1^+)	0.02	0.00
	^{10}Be(2_2^+)	1.1	0.92
	^{10}Be(3_1^+)	0.40	0.38
	^{10}Be(4_1^+)	0.08	0.10
	^{10}Be(2_3^+)	0.03	0.00
^{10}Be(0_1^+)	^{10}B(1$^+$)	2.9	2.5

B(GT) between ^{12}Be(0+) and ^{12}B(1+)
Exp: 0.59
Cal: 0.8

Kanada-En’yo et al.

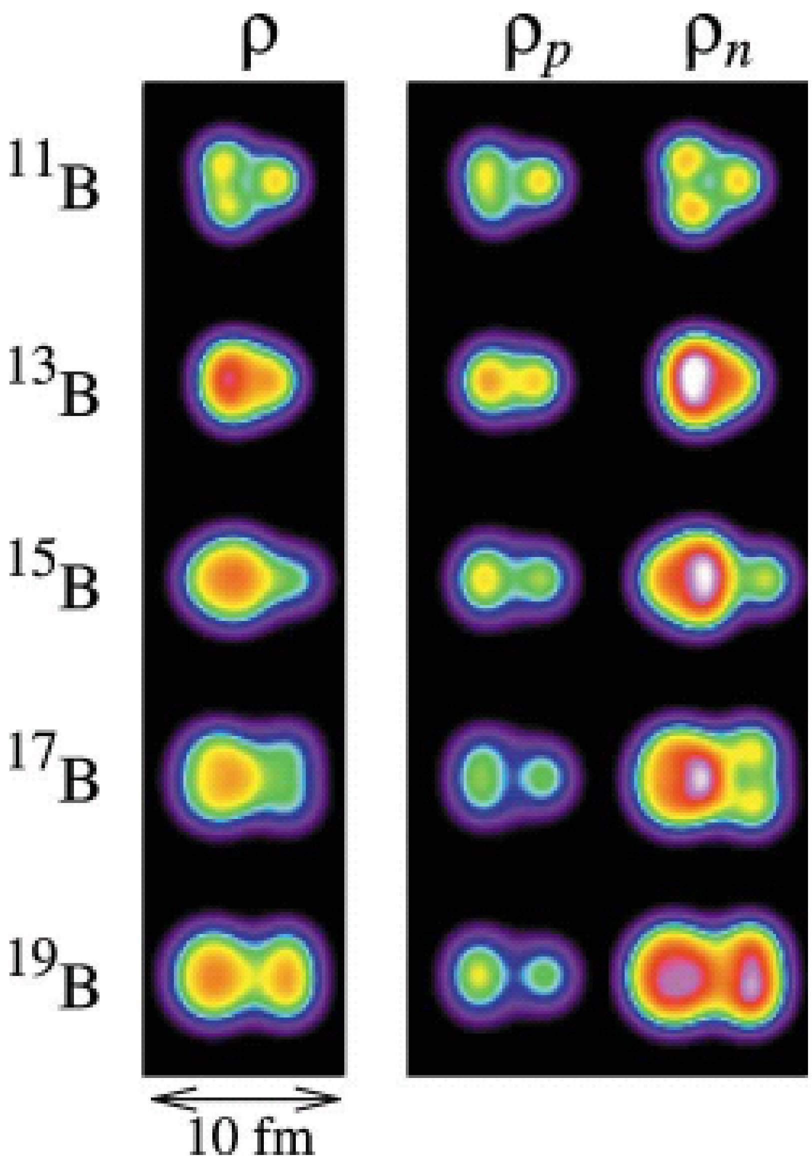

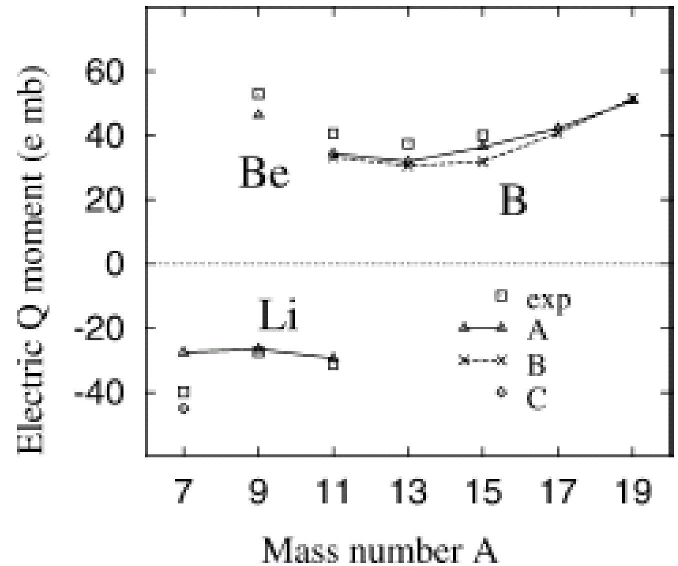

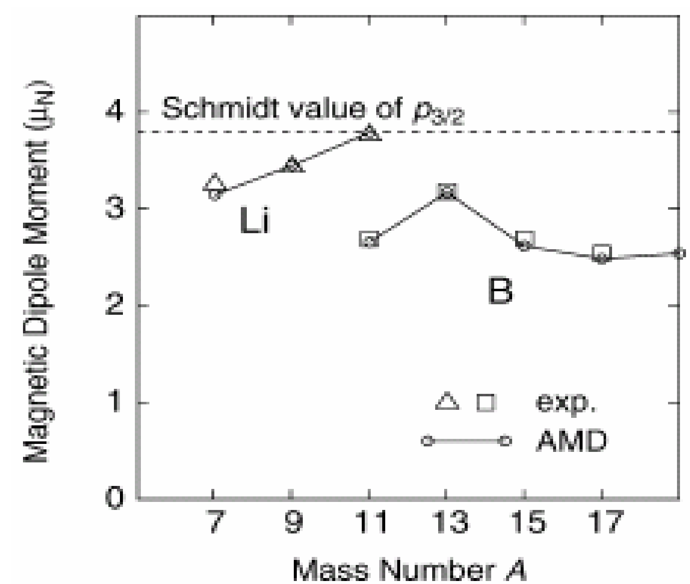

Kanada-En' yo et al.

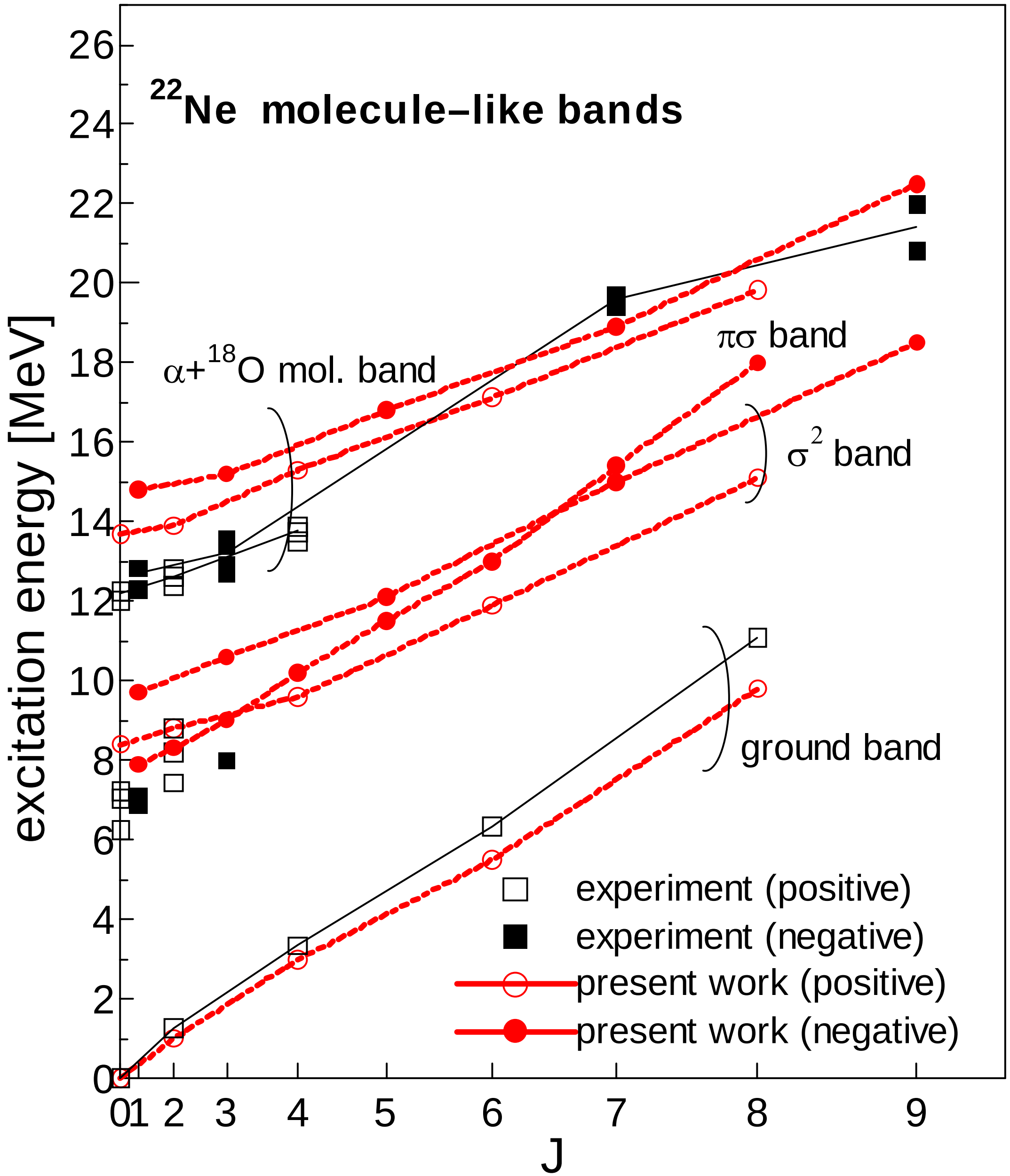

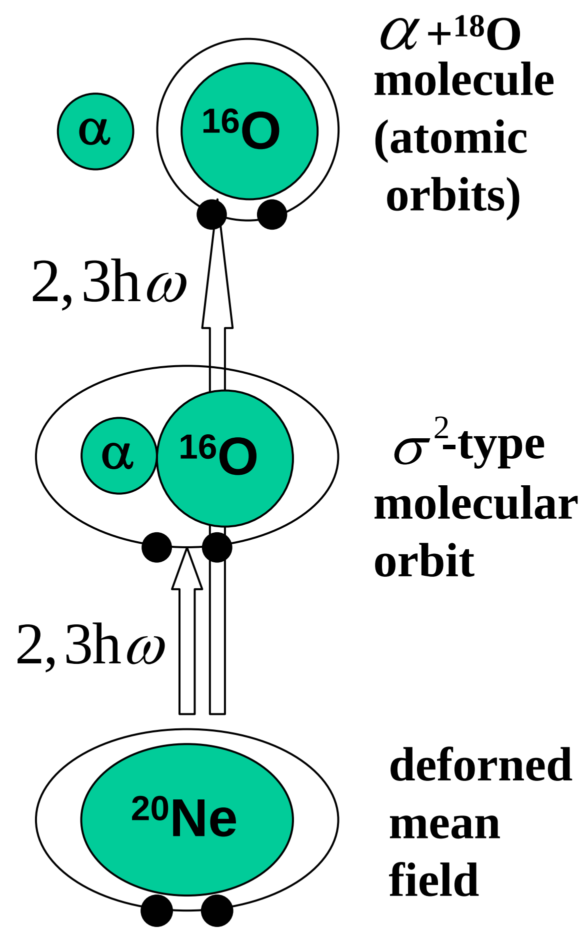

AMD calculation by M. Kimura

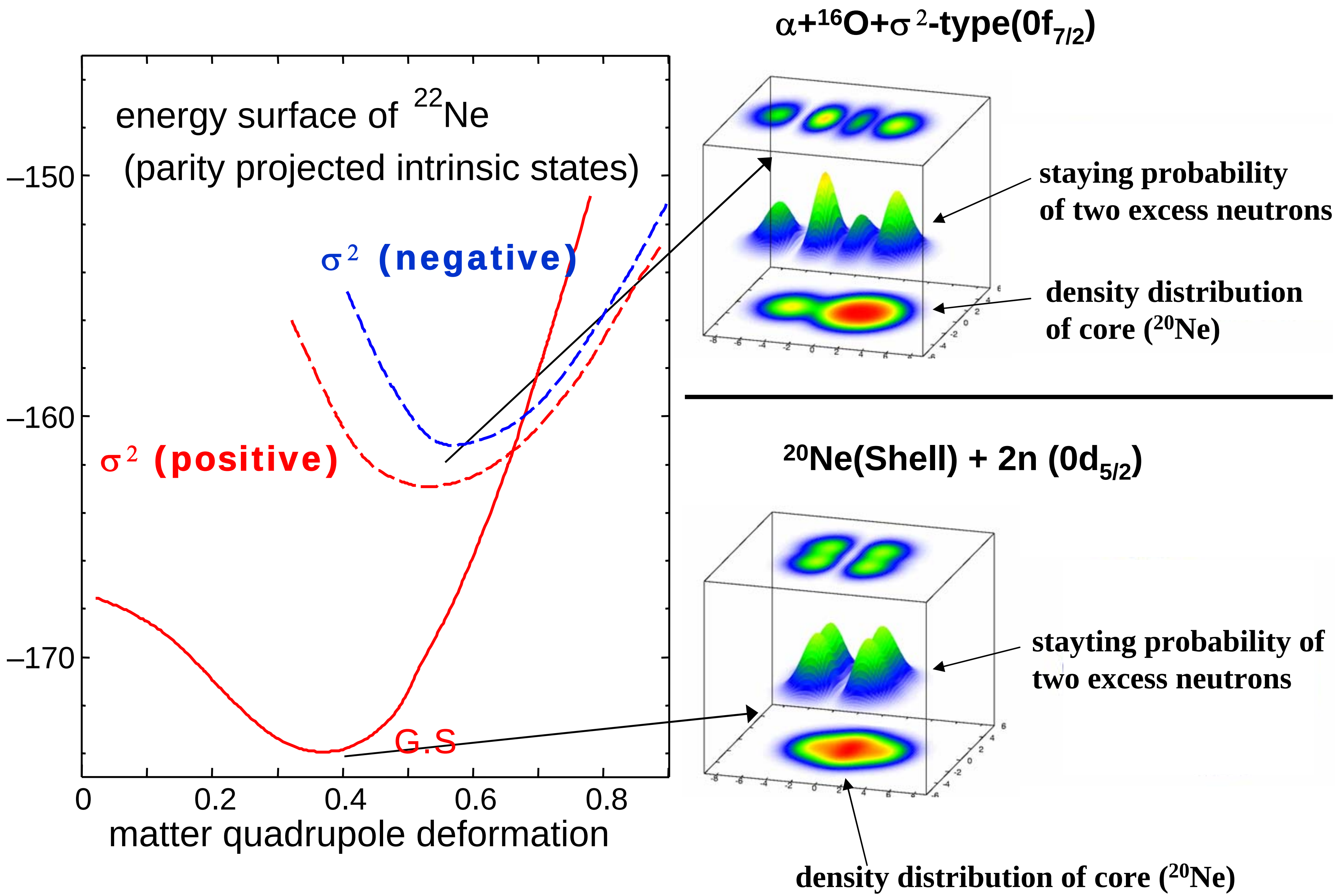

energy surface of 22Ne
(parity projected intrinsic states)
σ2 (negative)
σ2 (positive)
G.S
–150
–160
–170
0
0.2
0.4
0.6
0.8
matter quadrupole deformation
α+16O+σ2-type(0f7/2)
staying probability of two excess neutrons
density distribution of core (20Ne)
20Ne(Shell) + 2n (0d5/2)
stayting probability of two excess neutrons
density distribution of core (20Ne)

^{22}Ne spectra

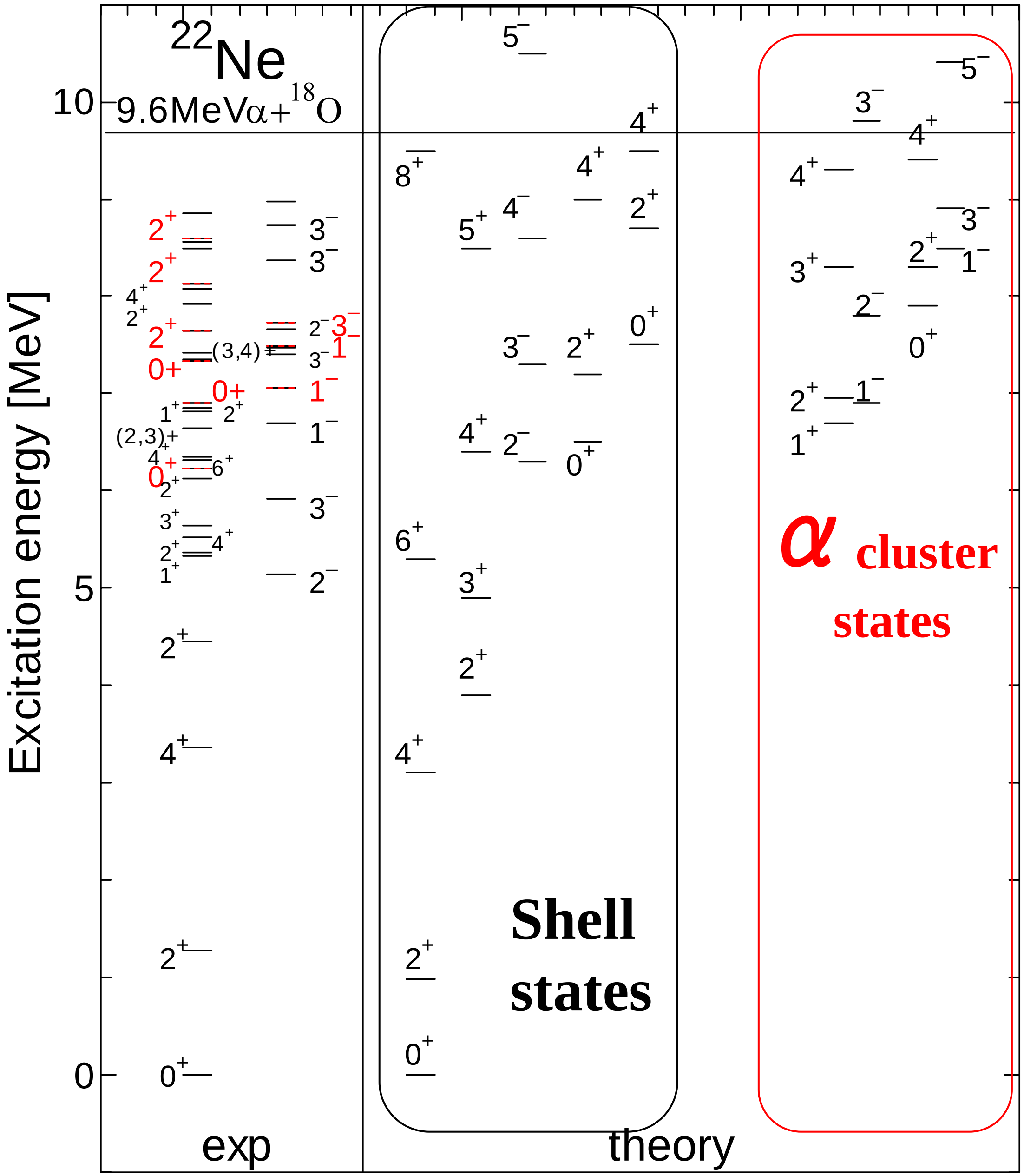

AMD calculation by M. Kimura

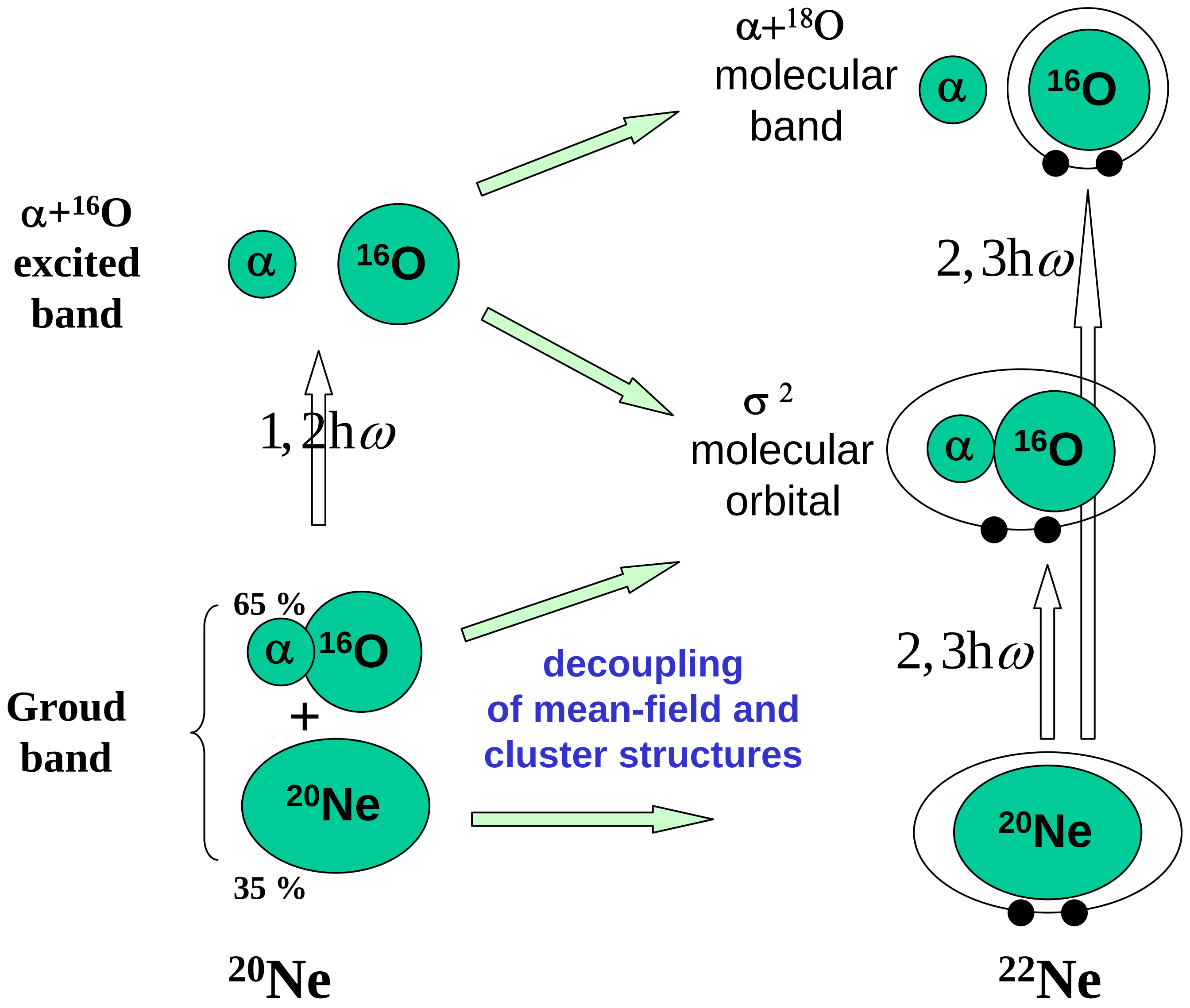
α+^{18}O
molecular
band
α
^{16}O
α+^{16}O
excited
band
α
^{16}O
$2, 3\hbar\omega$
$1, 2\hbar\omega$
σ ^{2}
molecular
orbital
α
^{16}O
65 %
α
^{16}O
+
^{20}Ne
35 %
Groud
band
decoupling
of mean-field and
cluster structures
$2, 3\hbar\omega$
^{20}Ne
^{20}Ne
^{22}Ne

3. Di-neutron cluster

^{11}Li

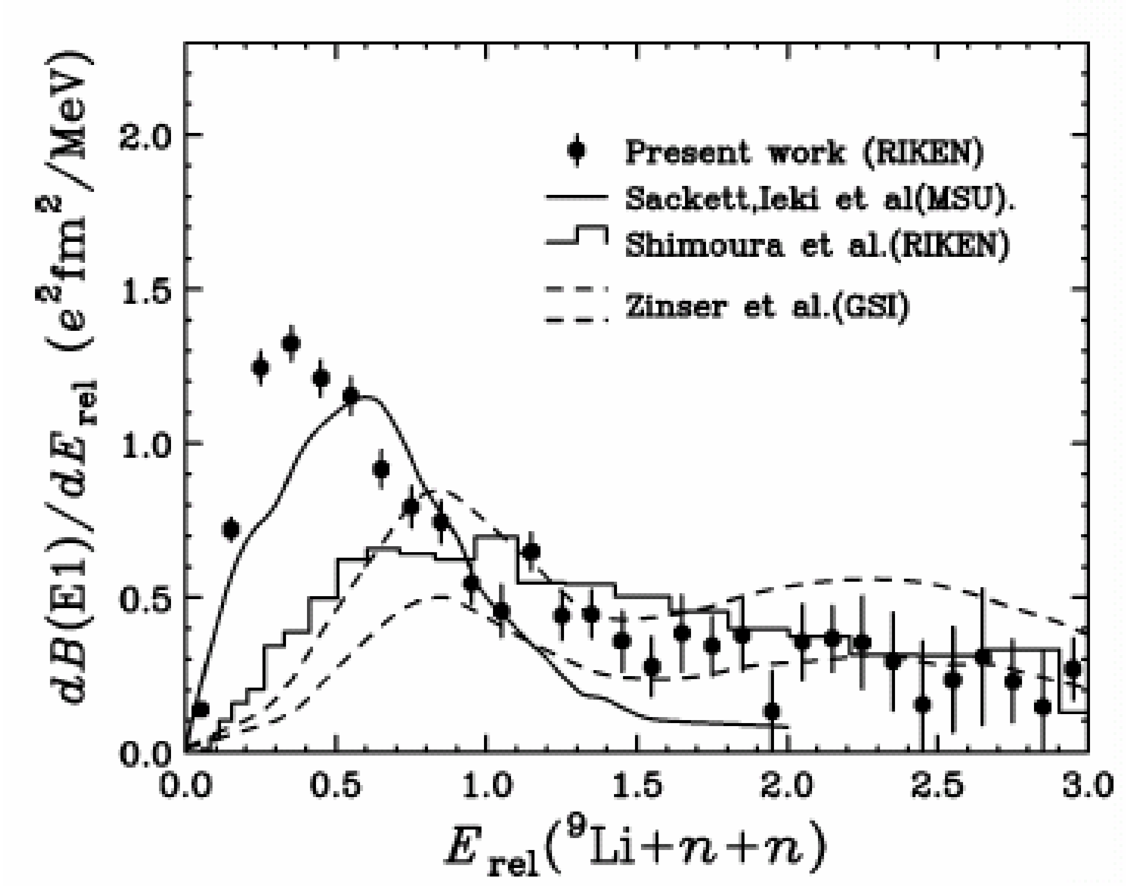

Present work:
T.Nakamura et al.
RIKEN Accel. Prog. Rep. 38

MSU@ 28MeV/nucleon
PRL 70 (1993) 730.
PRC 48(1993) 118.

RIKEN @ 43MeV/nucleon
PLB348 (1995) 29.

GSI @280MeV/nucleon
NPA 619 (1997) 151.

$$\frac{dB(E1)}{dE_x} \propto |\langle \exp(i\boldsymbol{q}\boldsymbol{r})|\frac{Z}{A}rY^1{}_m|\Phi_{gs}\rangle|^2$$

For di-neutron structure,
peak position is at **1.6 S_{2n}**
S_{2n}=0.66 MeV $\Longrightarrow$ **E_{peak}=0.47** MeV

Three-body model

G.F.Bertsch and H. Esbensen, Ann. Phys. (NY) 209, 327 (1991).
H. Esbensen and G.F.Bertsch, Nucl. Phys. A542, 310 (1992).
H. Esbensen, G.F.Bertsch, and K.Hencken, Phys.Rev. C56, 3054 (1999).
K.Hagino and H.Sagawa, Phys.Rev.C 72, 044321 (2005).

$$H = \hat{h}_{nC}(1) + \hat{h}_{nC}(2) + V_{nn} + \frac{\boldsymbol{p}_1 \cdot \boldsymbol{p}_2}{A_c m}.$$

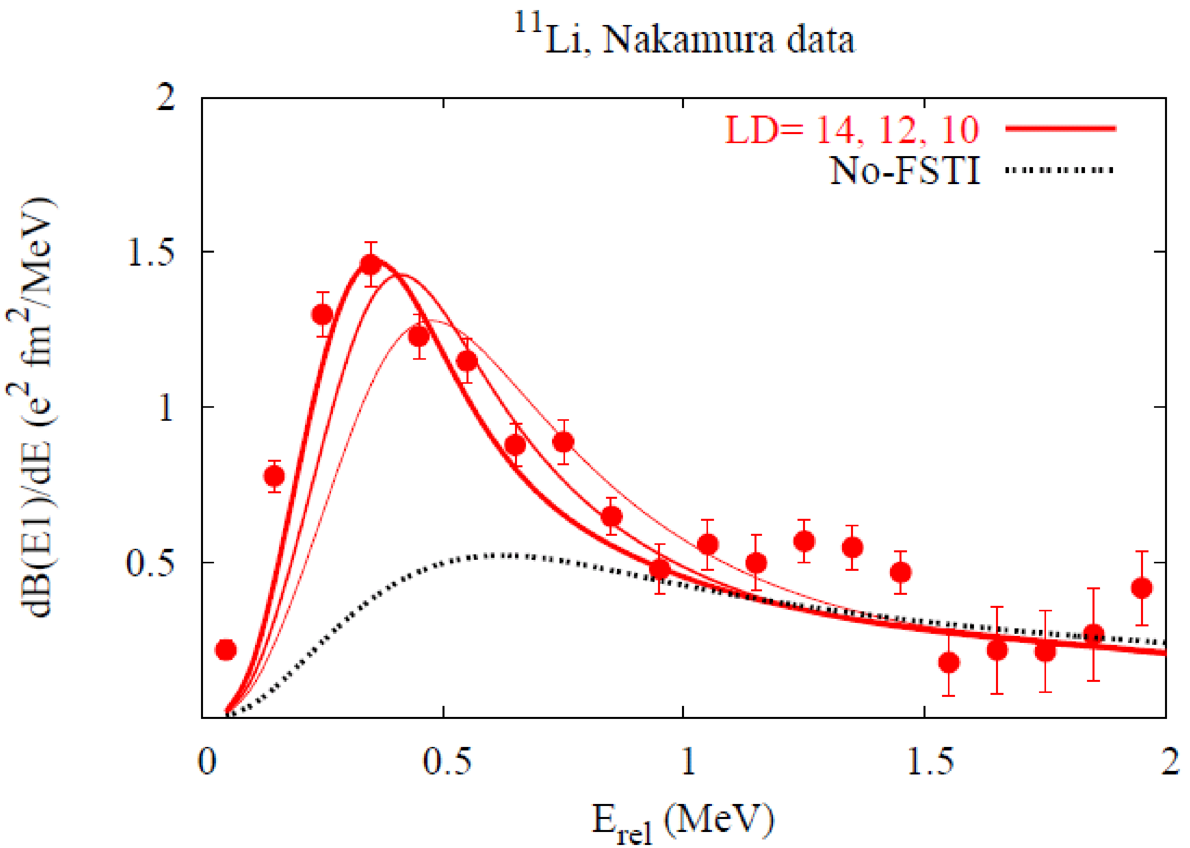

LD=14,12,10:
maximum angular momentum of single-particle states used to calculating $[1 + G_{1\mu}(0)V_{nn}]^{-1}$

H. Esbensen

^{11}Li

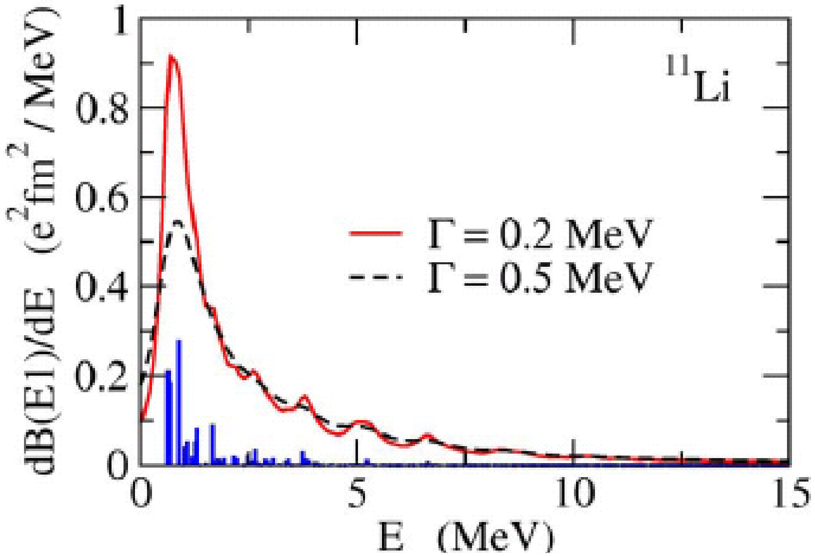

$$B(E1) = \sum_k \frac{\Gamma}{\pi} \frac{1}{(E - E_k)^2 + \Gamma^2} B_k(E1)$$

CAL:
Epeak = 0.66 MeV
B(E1) = 1.31 e2fm2 (E<3.3 MeV)

EXP:
Epeak ≈ 0.6 MeV
B(E1) = 1.5 ±0.1 e2fm2 (E<3.3 MeV)

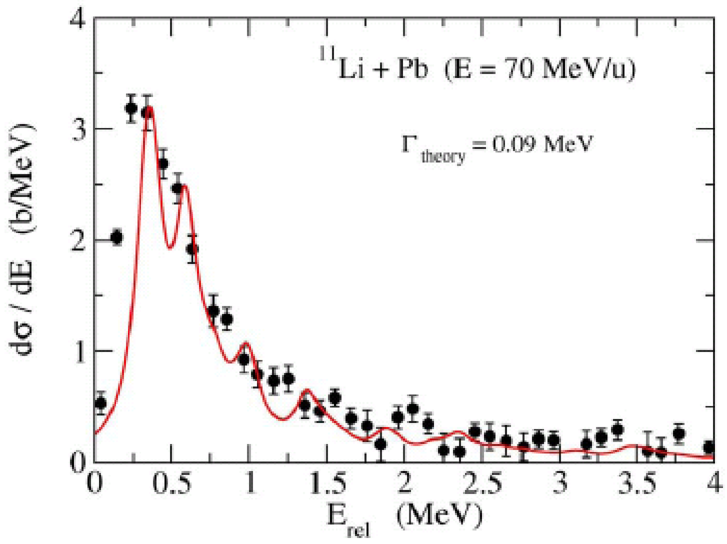

K.Hagino and H.Sagawa

^{11}Li

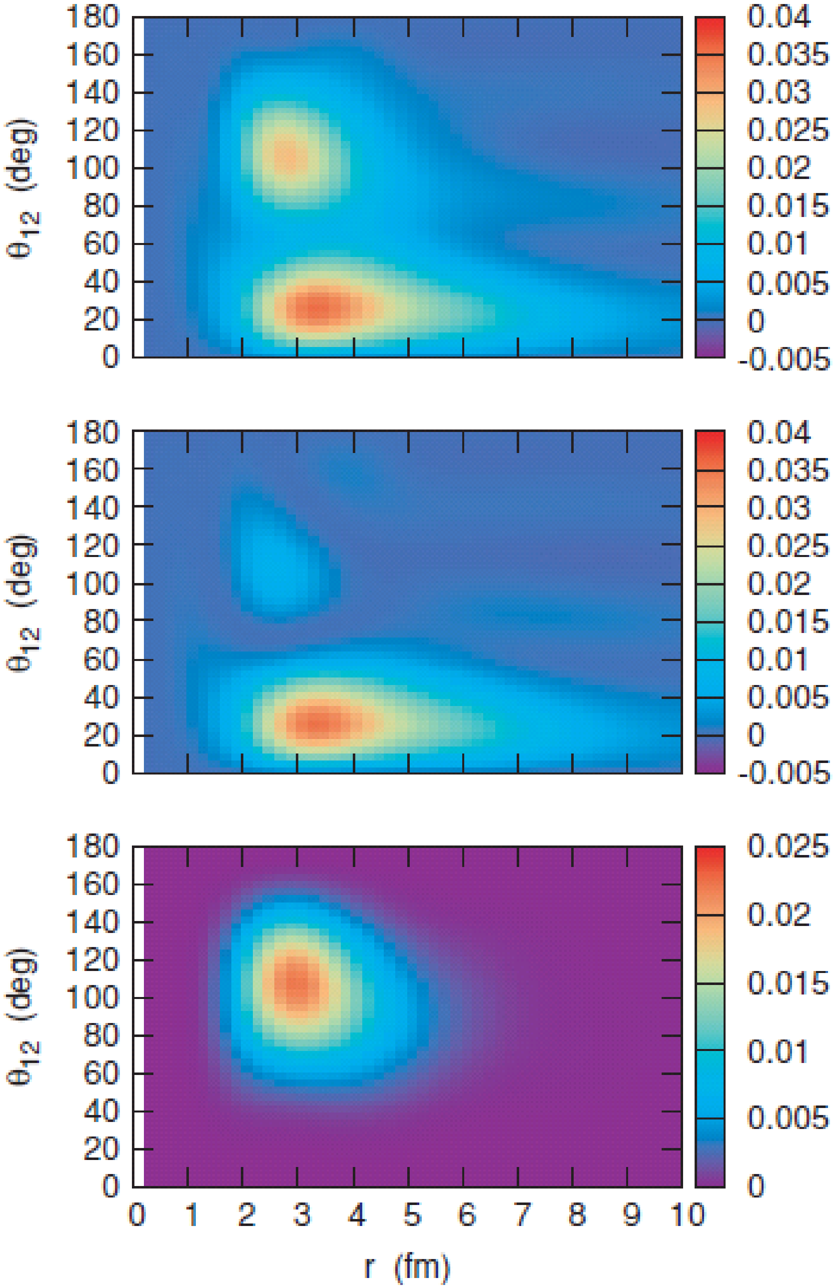

Total

S=0

$|\uparrow\downarrow\rangle$

S=1

$|\uparrow\uparrow\rangle$

or

$|\downarrow\downarrow\rangle$

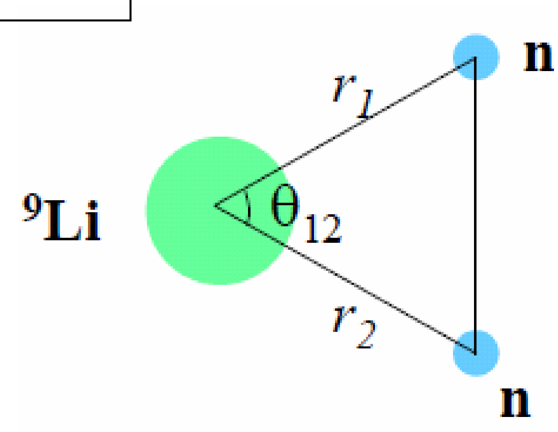

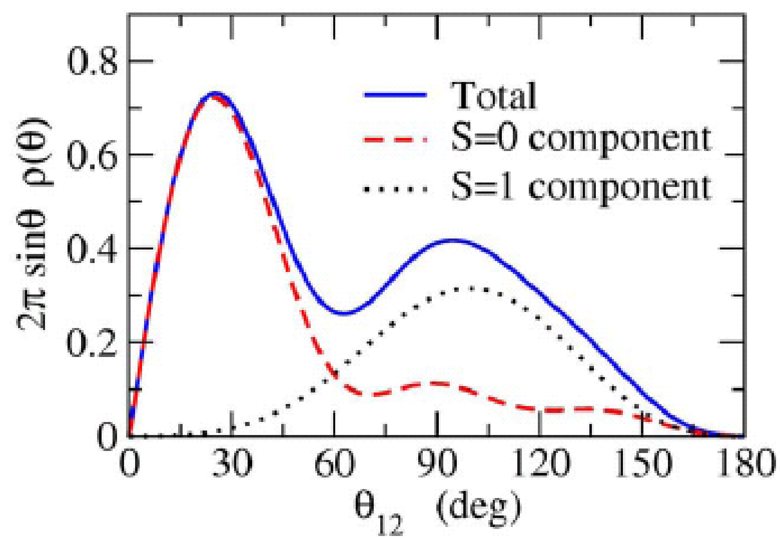

K.Hagino and H.Sagawa

$\rho_2(r_1, r_2, \theta_{12})$ for ^{11}Li

G.F.Bertsch, H.Esbensen
Ann.Phys. 209 (1991), 327.

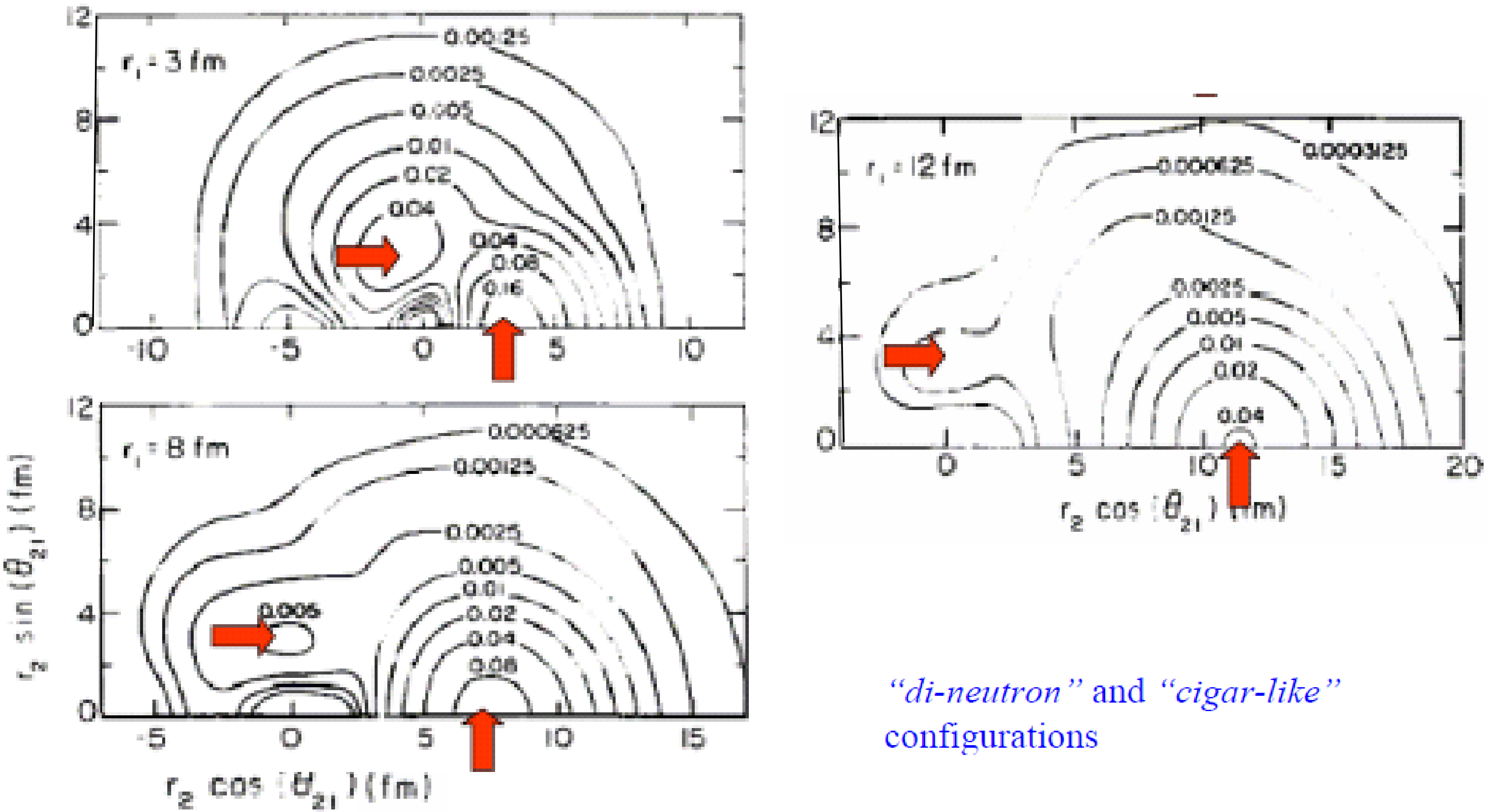

"di-neutron" and *"cigar-like"*
configurations

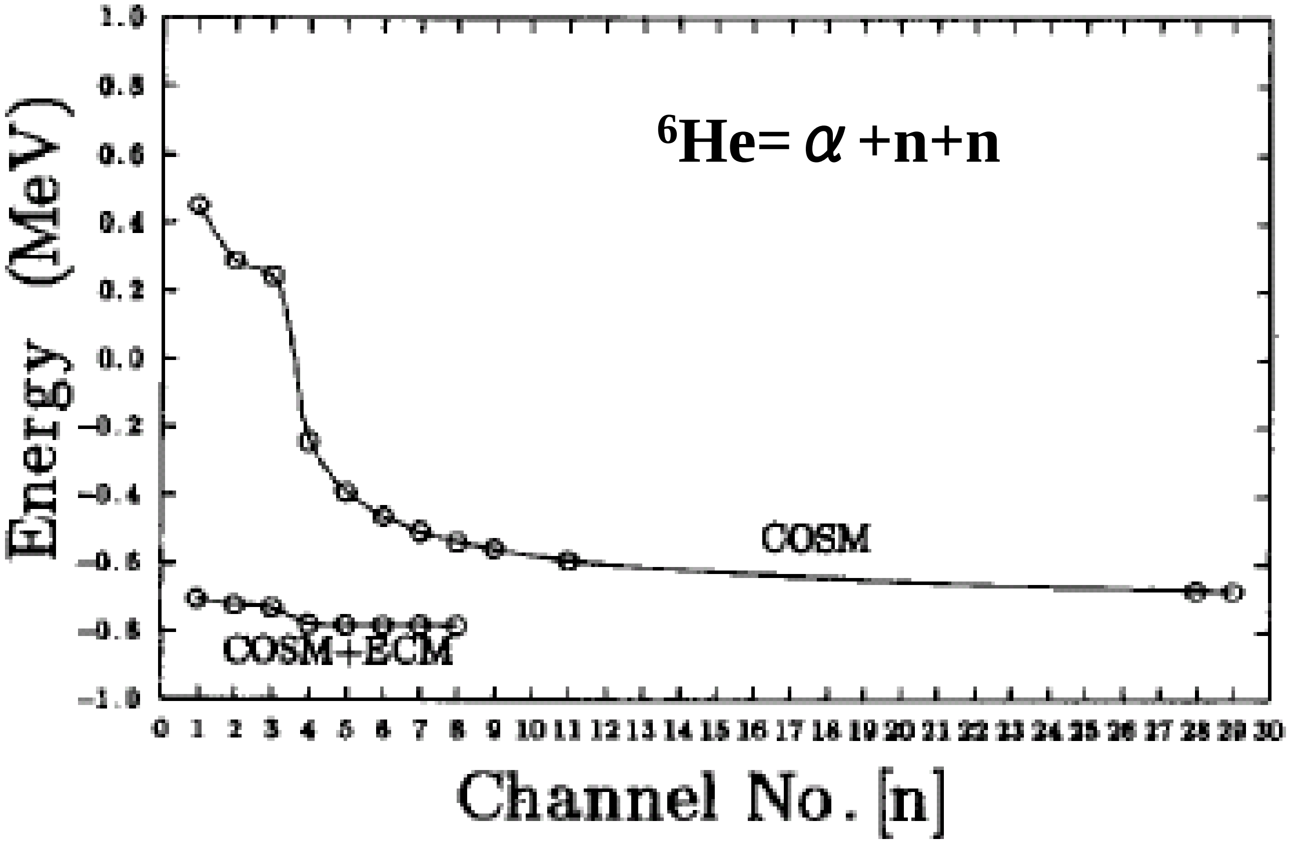

S. Aoyama,
S. Mukai,
K. Kato,
K. Ikeda

Prog.Theor.Phys. 93 (1995), 99.

Importance of di-neutron configuration

In ECM, only *l*=*L*=0 is employed.

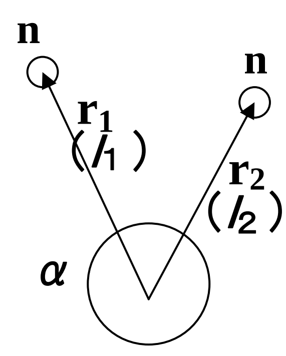

COSM

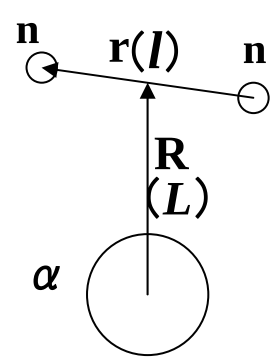

ECM

Table II. Channel configurations employed in the V-type basis functions for hybrid-TV model and COSM calculations together with the ground state energies calculated in several steps. The $l=L=0$ configuration is employed in the T-type basis functions of the hybrid-TV model.

Channel No.	Configurations	Hybrid-TV	COSM
[1]	$(p_{3/2})^2$	−0.709 MeV	0.451 MeV
[2]	$[1]+(p_{1/2})^2$	−0.724	0.288
[3]	$[2]+(s_{1/2})^2$	−0.732	0.243
[4]	$[3]+(d_{5/2})^2$	−0.780	−0.244
[5]	$[4]+(d_{3/2})^2$	−0.782	−0.392
[6]	$[5]+(f_{7/2})^2$	−0.784	−0.463
[7]	$[6]+(f_{5/2})^2$	−0.784	−0.510
[8]	$[7]+(g_{9/2})^2$	−0.784	−0.538
[9]	$[8]+(g_{7/2})^2$		−0.559
[10]	$[9]+(h_{11/2})^2$		·
[11]	$[10]+(h_{9/2})^2$		−0.593
[12]	$[11]+(i_{13/2})^2$		·
[13]	$[12]+(i_{11/2})^2$		·
[14]	$[13]+(j_{15/2})^2$		·
[15]	$[14]+(j_{13/2})^2$		·
·	·		·
·	·		·
·	·		·
[28]	$[27]+(l=14,\ j=29/2)^2$		−0.681
[29]	$[28]+(l=14,\ j=27/2)^2$		−0.682

HFB calculation

M.Matsuo et al.

PRC 71, 064326(2005)

Di-neutron correlation in the medium-mass region

2-body correlation density (spin anti-parallel)

$$\rho_2^{corr}(\vec{r}'\uparrow;\vec{r}\downarrow) = \sum_{i\neq j}\delta(\vec{r}-\vec{r}_i)\delta_{\sigma_i\uparrow}\delta(\vec{r}'-\vec{r}_j)\delta_{\sigma_j\downarrow} - \rho_1(\vec{r}'\uparrow)\rho_1(\vec{r}\downarrow)$$

$$\approx |\Psi_{pair}(\vec{r}\uparrow,\vec{r}'\downarrow)|^2$$ wave function of neutron pair

HFB with SLy4

Mix-type DDDI

^{84}Ni

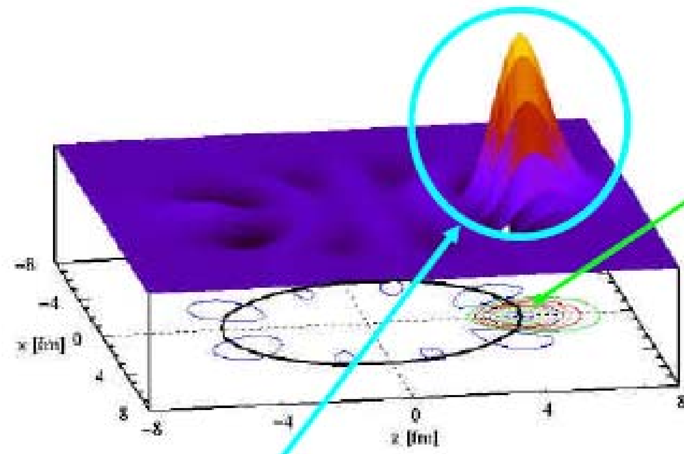

one neutron fixed at $\vec{r}'$

di-neutron correlation

Strongly correlated at short relative distances |r-r'| < 2-3fm

Di-neutron probability

relative weight for $|r-r'|<r_d$

$P(r_d) = 0.27 \quad (r_d=2)$

Di-neutron correlation is enhanced in the low-density skin region

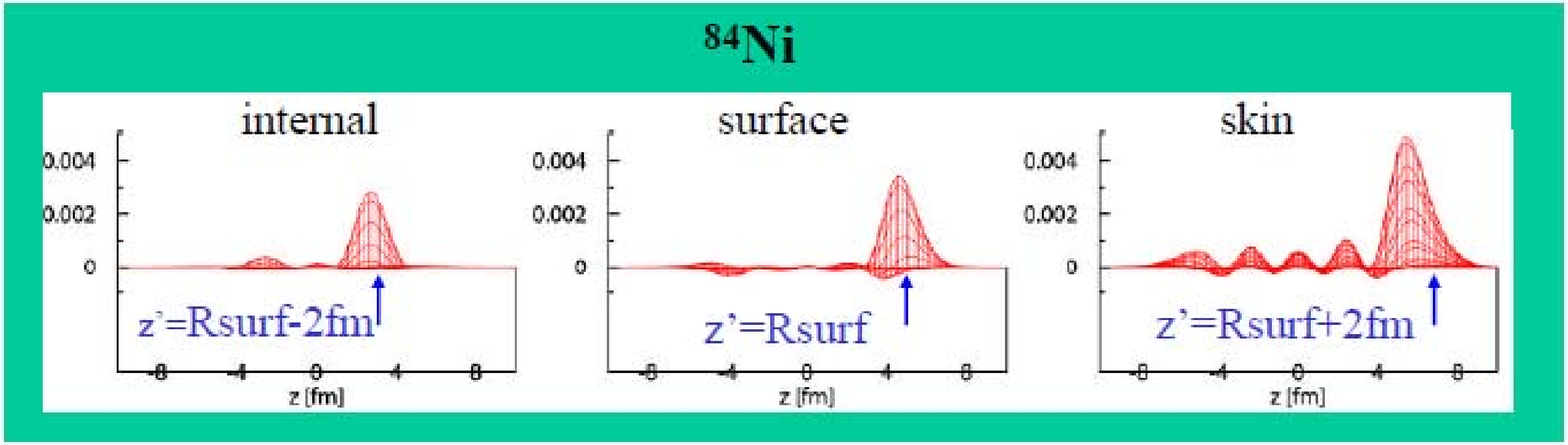

Di-neutron probability $P(r_d)$ (relative weight within r_d=2(3)fm)

	Internal	surface	skin
^{22}O	0.32	0.48	0.47
^{58}Ca	0.39	0.53	0.59
^{84}Ni	0.32	0.49	0.47

M.Matsuo et al.

M.Matsuo et al.

Configuration mixing: High-L orbits

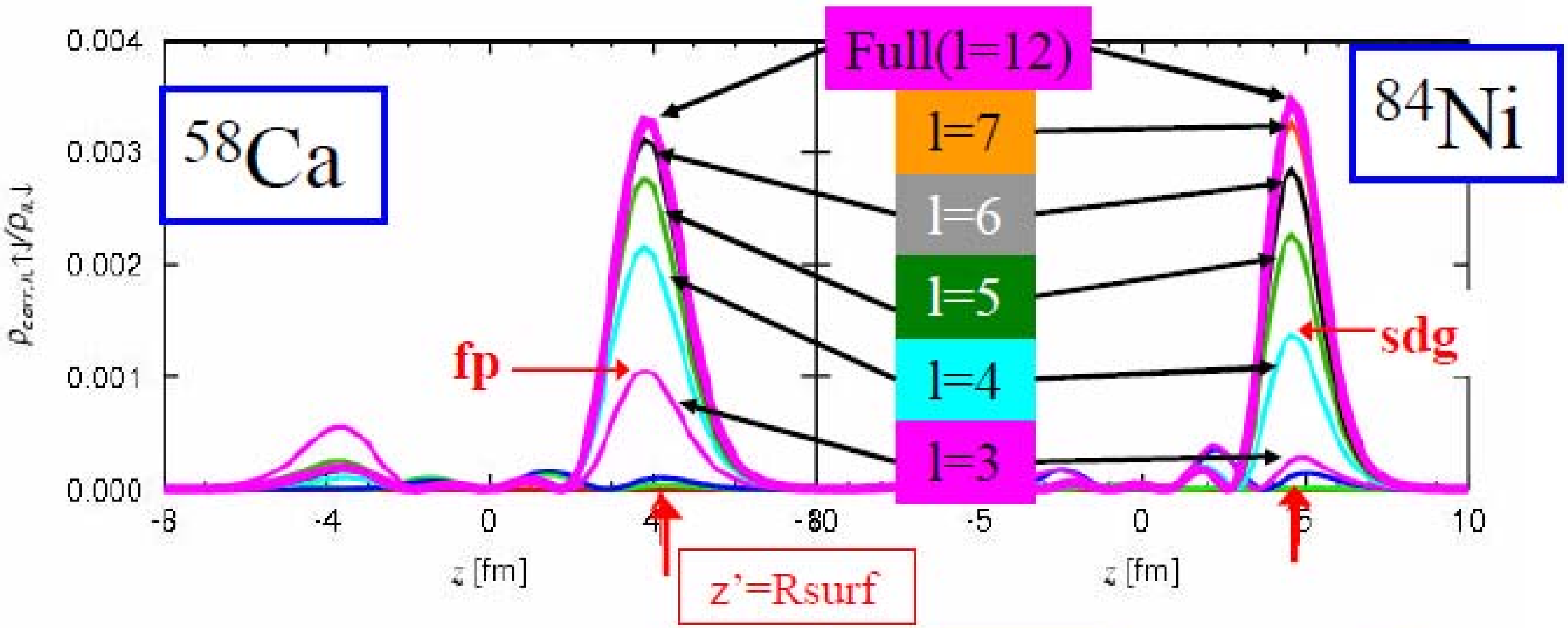

The coherent superposition of
high-L oribts *l*=3-8
in the continuum
forms the di-neutron correlation

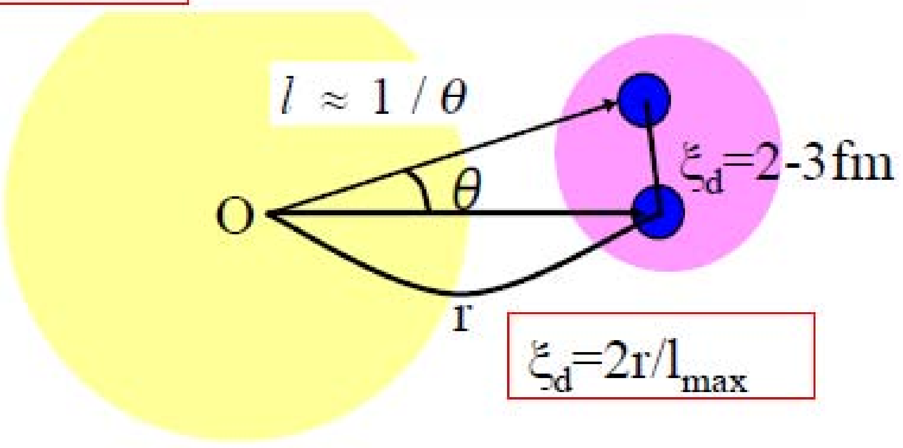

4. Multi-cluster core + neutrons

Excess neutrons stabilize D_{3h} symmetry of 3α

N. Itagaki, T.Otsuka, K.Ikeda, S.Okabe
PRL 92 142501(2004)

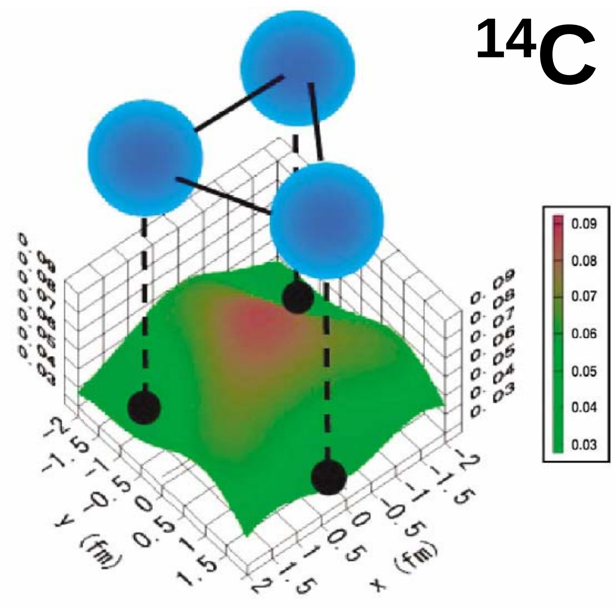

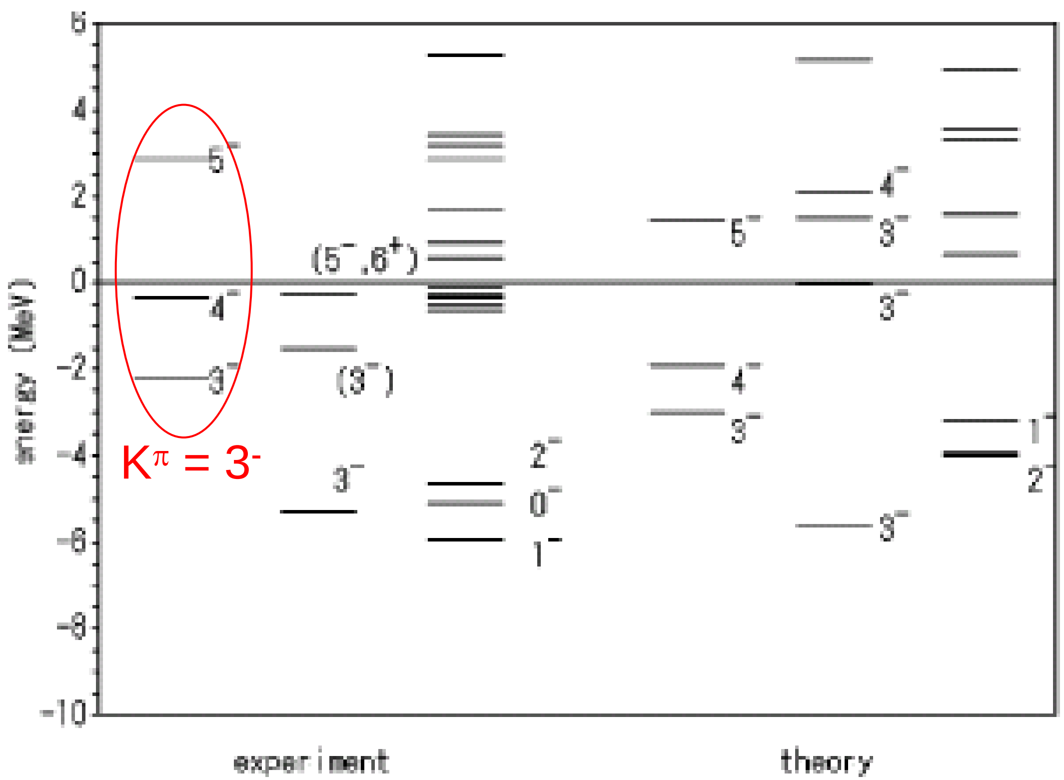

Observed levels

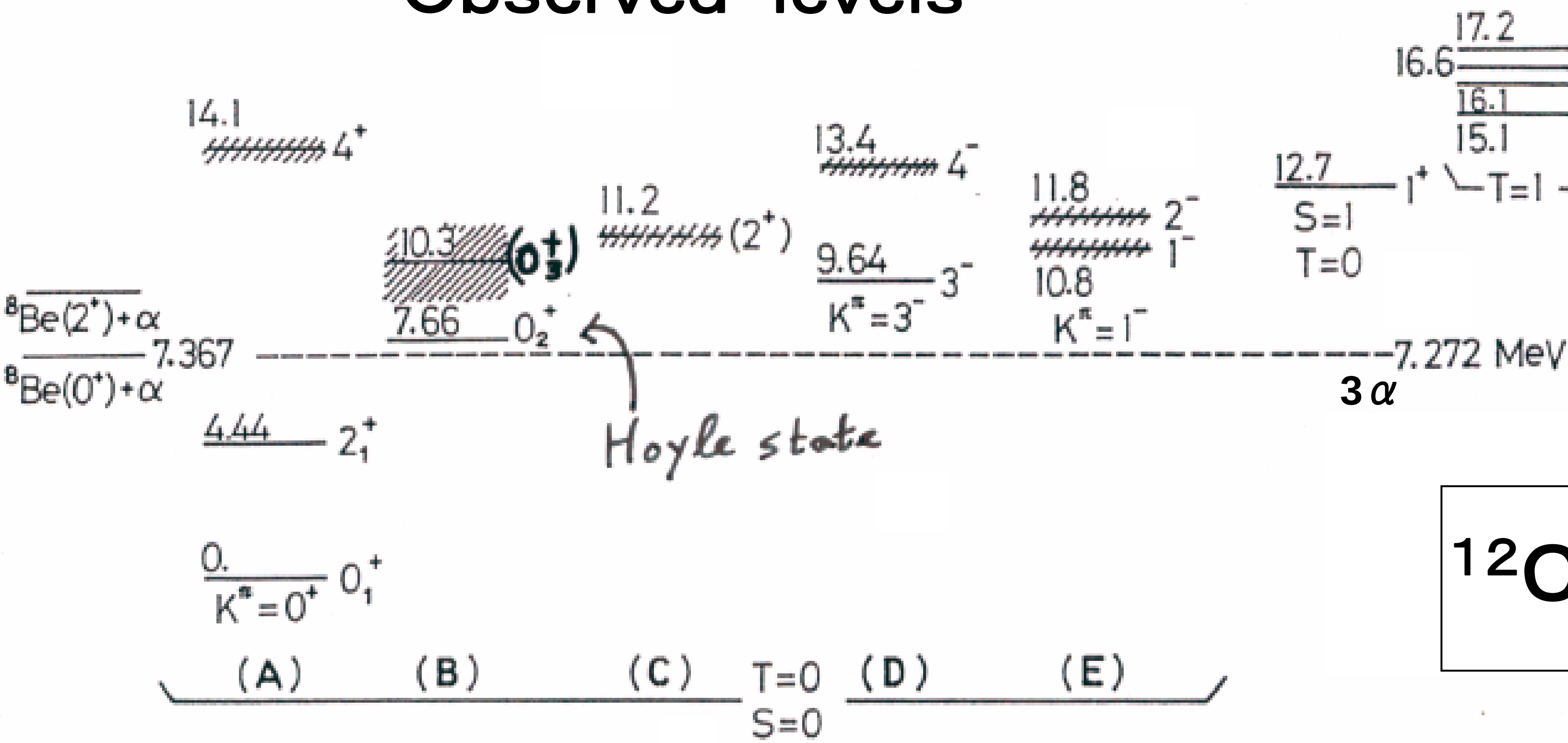

^{12}C

Recent RCNP experiments

M.Itoh, et al.,

N.P.A.738,268,(2004)

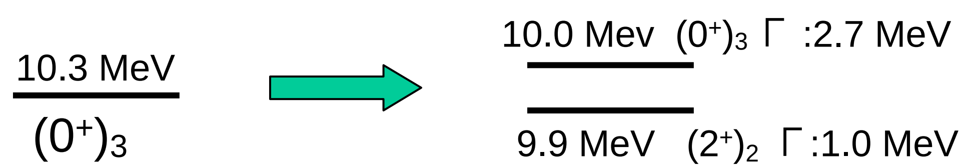

Excess neutrons stabilize linear chain of α

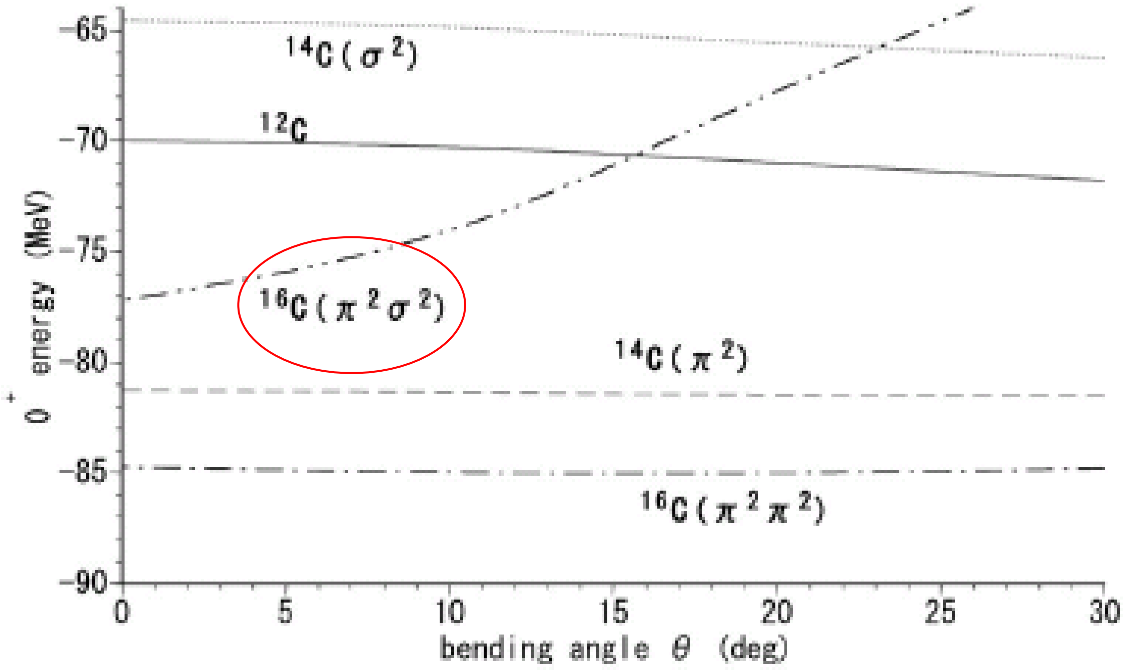

N. Itagaki, S. Okabe,
K.Ikeda, I. Tanihata,
P. R C 64, 014301 (2001)

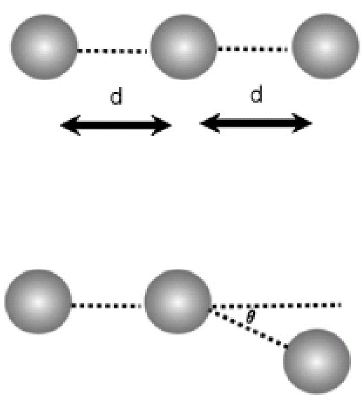

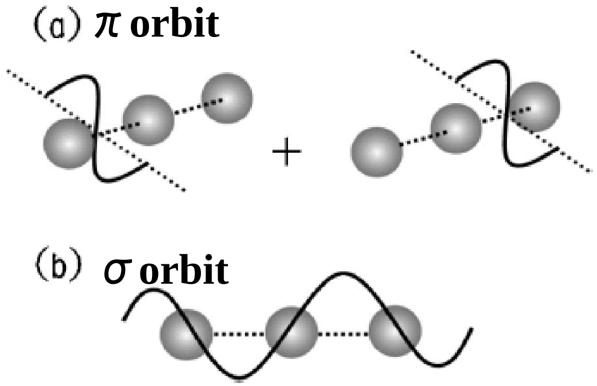

5. Summarizing discussion

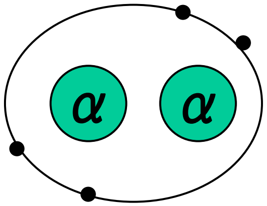

○ **Di-cluster + neutrons**

1. **Neutrons are described by molecular orbits**

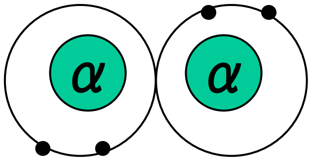

molecule

2. **Neutrons are described by atomic orbits**

○ **Di-neutron cluster**

1. **^{11}Li = ^{9}Li + di-nuetron,**
   probably ^{6}He = α + di-neutron

2. **di-neutron condensation in neutron skin (dilute neutron matter)**
   HFB calculation

○ **Multi-cluster stabilized by excess neutrons**

1. **Triangle structure of 3α**
2. **Linear chain structure of α clusters**

○ **Clustering in dilute nuclear matter**

1. **Di-neutron condensation in neutron skin/halo of neutron-rich nuclei**
2. **α cluster condensation in near-proton-dripline nuclei ?**

   α cluster condensation in neutron-richer nuclei ?

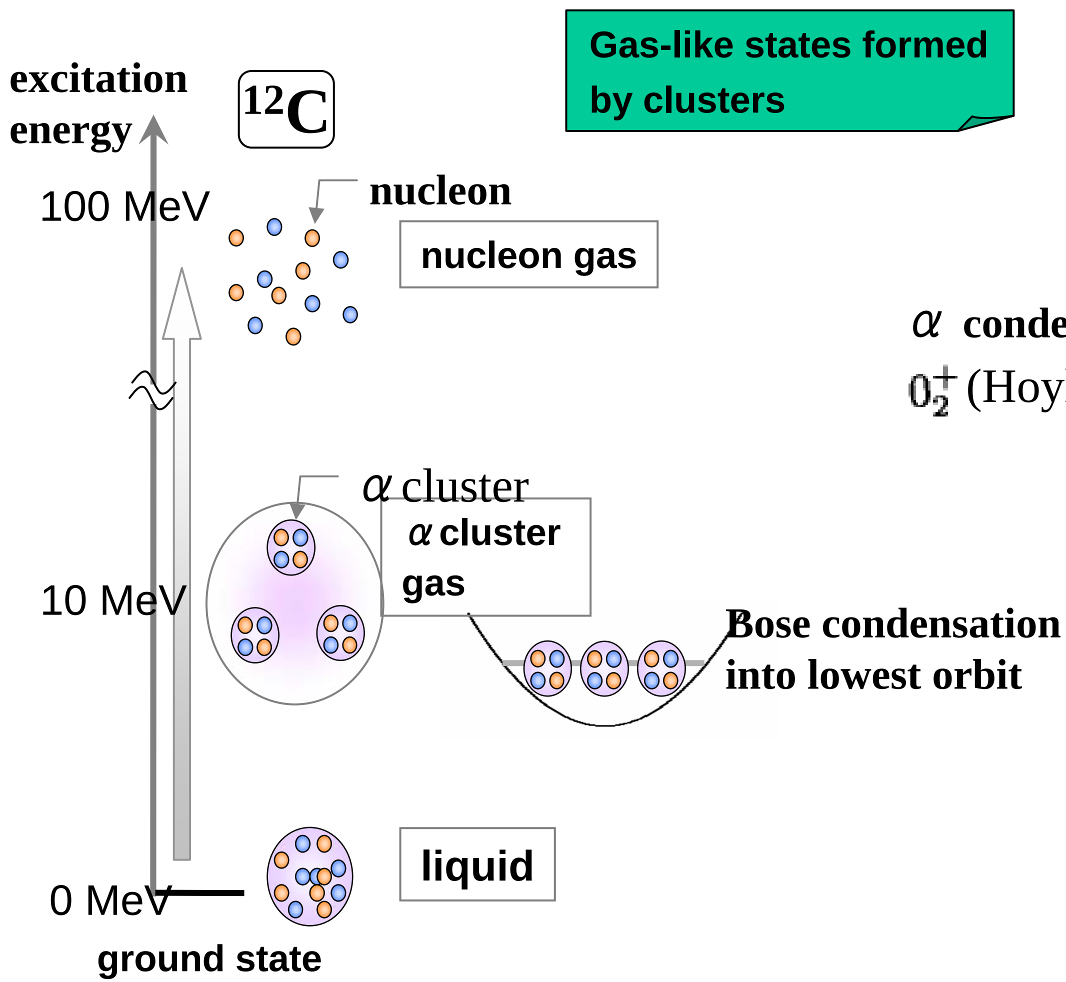

α condensed state

0_2^+ (Hoyle state)

Y. Funaki,
A. Tohsaki,
H. Horiuchi,
P. Schuck,
G. Roepke

Dilute nuclear states

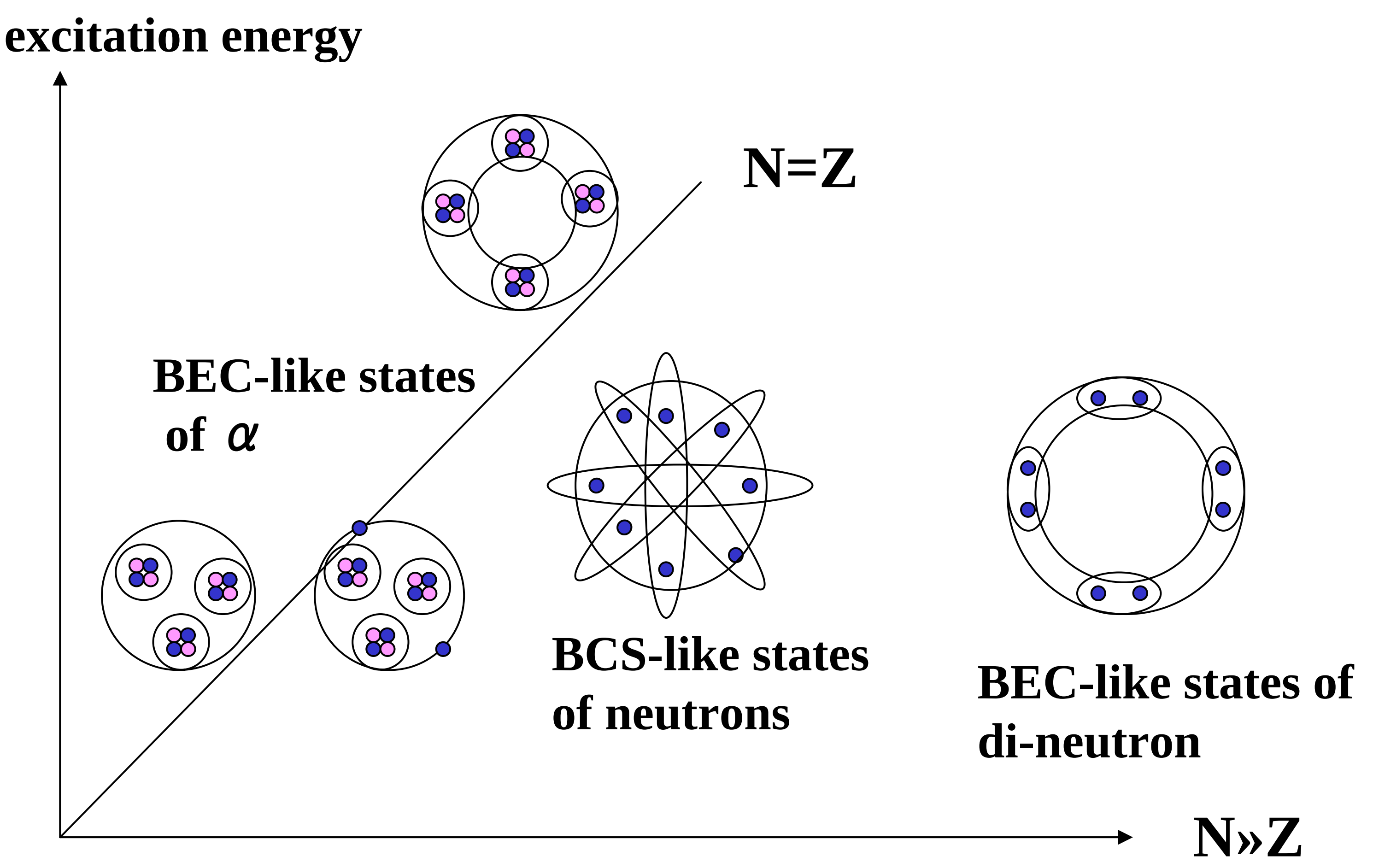

The studies we discussed serve to elucidate

Richness of nuclear dynamics :

- ◇**New dynamics near driplines,**
- ◇**New dynamics in excited states,**

an example: no-core shell model cannot reproduce the second 0+ states and related states in ^{12}C

Various kinds of dynamics: mean-field dynamics,
strong correlation dynamics,
clustering dynamics,

Advantages of RIA compared with RIBF (RIKEN)

Variety of energies of exotic beams

post acceleration of exotic nuclei

in addition to in-flight exotic fragments

one example, fragmentation experiments of B isotopes to check their

Li-He molecular structure

30-50 MeV/nucleon is desirable for B beams

(H.Takemoto, A.Ono, & H.H. P.R.C63, 034615('01), P.T.P. 101, 101('99), AMD calculation of fragmentation)

Large reaction yields by exotic beams

at least more than 400 MeV/nucleon .... RIA

at most less than 350 MeV/nucleon ....RIBF

necessary for more detailed studies of

excited states of exotic nuclei

Observed levels of ^{12}C

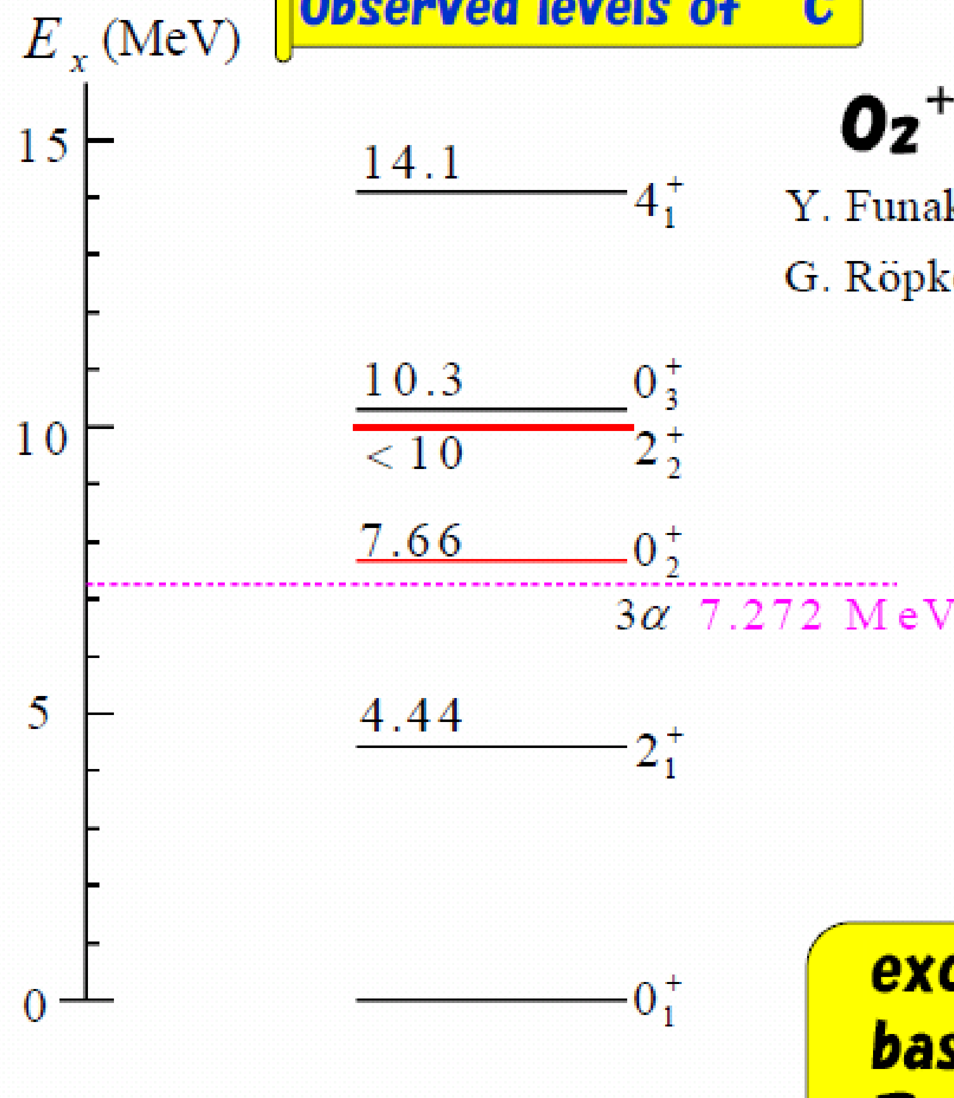

0_2^+ state : 3α condensed state

Y. Funaki, A. Tohsaki, H. Horiuchi, P. Schuck, and G. Röpke, Phys. Rev. C 67 (2003) 05130610

2_2^+ state :

$E = 9.9 \pm 0.3$ MeV

$\Gamma = 1.0 \pm 0.3$ MeV

$^{12}C(\alpha, \alpha')$

M. Itoh et al., Nucl. Phys. A 738 (2004) 268-272

excitation mode
based on α condensate
2α particles : S-orbit
1α particle : D-orbit

0_2^+ state

	Exp.	Theor.
Excitation energy (MeV)	7.65	7.74
Width (eV)	8.7±2.7	7.7
$M(0_2^+ \to 0_1^+)$ (fm^2)	5.4±0.2	6.7
$B(E2: 0_2^+ \to 2_1^+)$ ($e^2 fm^4$)	13±4	5.6

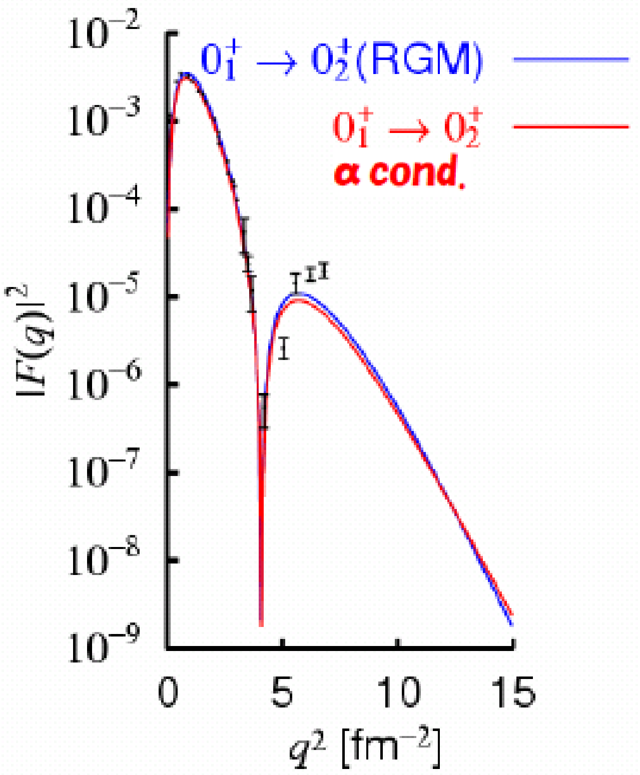

2_2^+ state

Exp	E=9.9±0.3 MeV Γ=1.0±0.3 MeV
α cond. w. f. + ACCC	E=9.38 MeV Γ=0.64 MeV